Effects of Lateral Distribution of Heavy Vehicles on Fatigue Cracks of Concrete Pavements

Tatsuo NISHIZAWA, Ishikawa College of Technology
Yasuo KAJIKAWA, Kanazawa University
Tadashi FUKUDA, Tohoku University

INTRODUCTION

Lateral distribution of heavy vehicles affects largely on the fatigue cracks of concrete pavements. When the width of concrete slab is small, wheels of heavy vehicles tend to pass near its longitudinal joint and in this case transverse crack would occur from the joint edge. On the other hand, where the width of slab is large, longitudinal cracks occurring from the transverse joint would be more predominant. Therefore, in the guides for the design of the concrete pavement [1,2] the lateral distribution of wheels of large vehicles is taken into account. However, data on the lateral distribution of wheels is limited because of the difficulty of the data acquisition. In this study, we developed Traffic Load Auto Measuring System (TLAMS) [3], which can monitor traffic flow by recording wheel positions, speeds as well as headways. Using the lateral distribution of wheels obtained by TLAMS, fatigue analysis of concrete pavements was conducted and the effects of lateral distribution of wheels were investigated in this study.

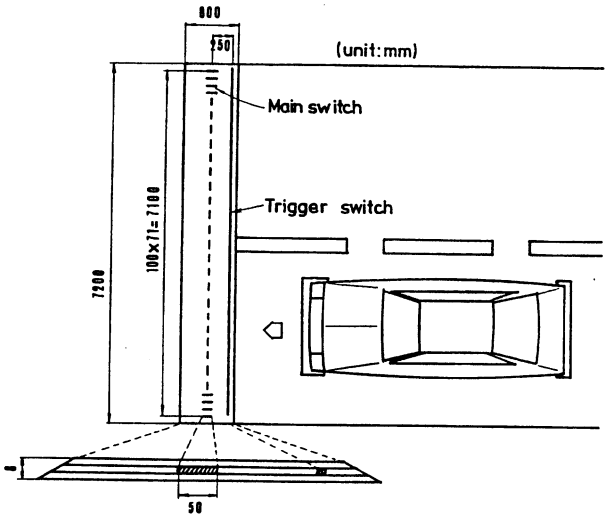


Figure 1: Measurement by TLAMS

MEASUREMENT OF LATERAL DISTRIBUTION OF WHEELS

Outline of TLAMS

Small switch sensors are attached at the surface of a rubber mat at regular intervals as shown in Figure 1. In the measurement, the rubber mat is placed transversely on a roadway. As a vehicle passes over the mat, some switch sensors are touched by its wheels and activated. Then, the position and the width of tire can be measured. From the passing time between the trigger switch and the main switch, speed of the vehicle can be also determined.

Figure 2 shows the block diagram of TLAMS. The system consists of a switch mat, a data logging box and a personal computer for data processing. Modems are connected by optical fibers for long distance communication. The equipments of the system are so compact that they can be transported by a station wagon. Installation or removal of the mat takes only a few minutes. Thus, measurement can be done at any point where a small spot is available for parking the station wagon.

Figure 3 shows an example of data obtained by the sys-

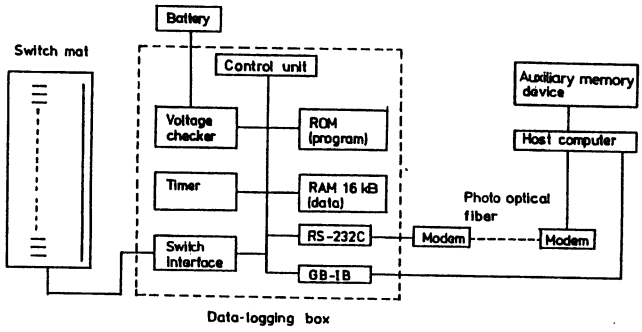


Figure 2: Block diagram of TLAMS

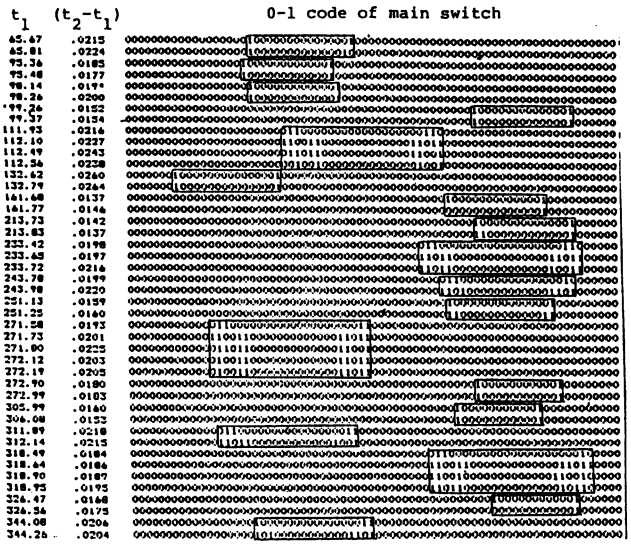


Figure 3: Data of TLAMS

tem. One set of the data for one axle consists of 72 bits, which correspond to small 72 switches, 24 bits for the passing time, t_1, when the wheels touch the trigger switch, and 16 bits for the passing period, $(t_2 - t_1)$, where t_2 is a time when wheels touch the main switches. In the system, time is counted by a real-time clock with an accuracy of 2^{-15} seconds.

The data is processed according to the flow chart shown in Figure 4. All vehicles are classified into seven types by means of the patterns of tread, tire, axle number and wheel base as shown in Figure 5. In this study, heavy vehicle is defined as one of which wheel base is more than $4.2m$.

Modeling of lateral distribution of wheels

Measurements by TLAMS were conducted at eleven road sites in Japan. Figure 6 shows some examples of the measurement results at two sites with two lanes in one direction. The results are shown for all vehicles and heavy vehicles separately. In the figure, ordinate shows frequency and abscissa is the distance form the left side end of the switch mat to the center of wheel. Vertical lines in the figure indicate the places of lane mark. Since the left side of the switch mat was coincided with the shoulder in the measurements, the left side and right side of the figures mean the shoulder and the center of the road, respectively. From the results, it is concluded that the lateral distributions of wheels could be approximated to be the normal distribution and its parameters depend on lane width.

Figure 7 shows the relationships between average and standard deviation of the distance between the right lane mark and the center of the tire of right wheel. From the figure, it can be seen that there are relationships between the parameters and lane width. The following equations were derived from regression analysis.

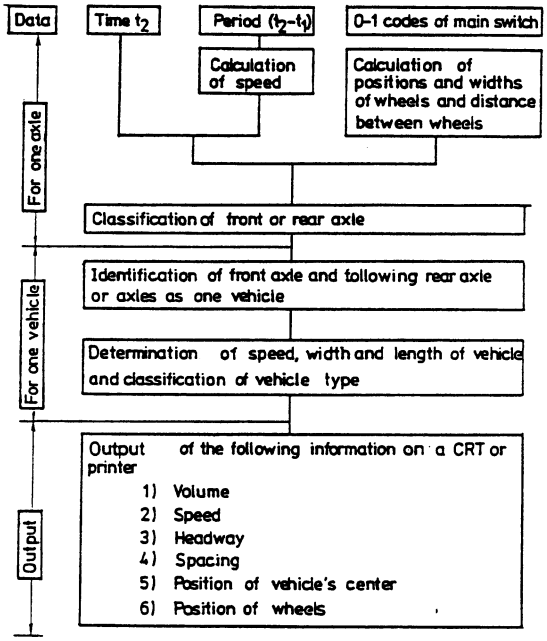


Figure 4: Flow chart for data processing

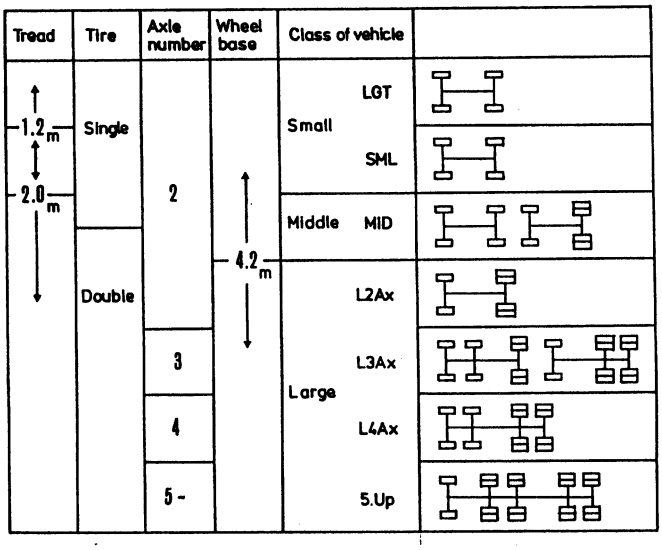


Figure 5: Classification of vehicle

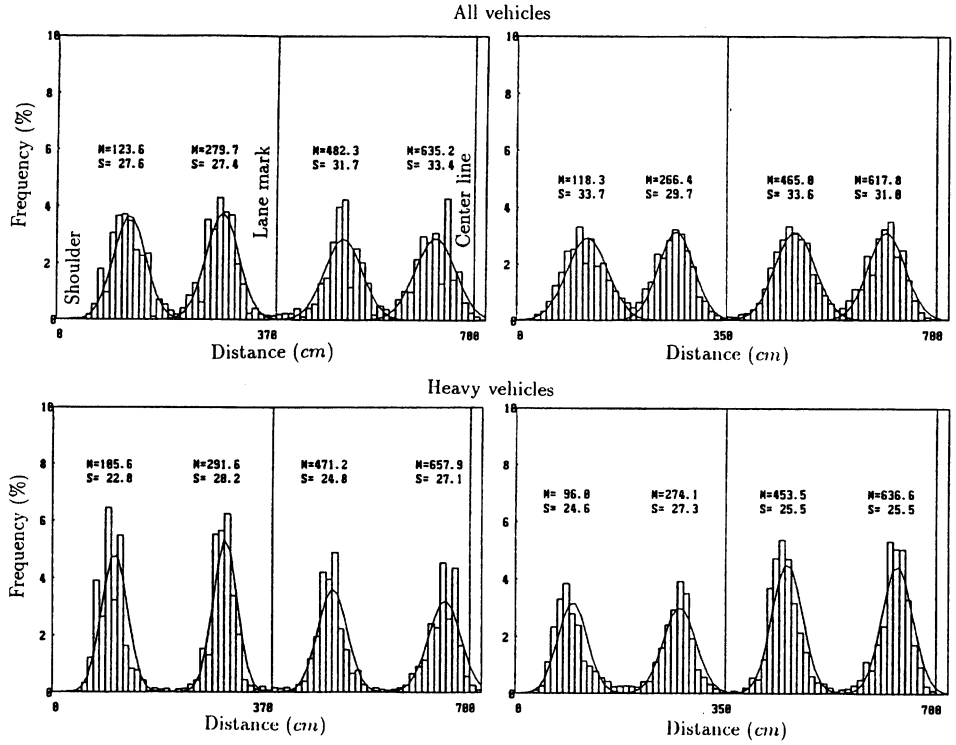


Figure 6: Examples of measurement by TLAMS

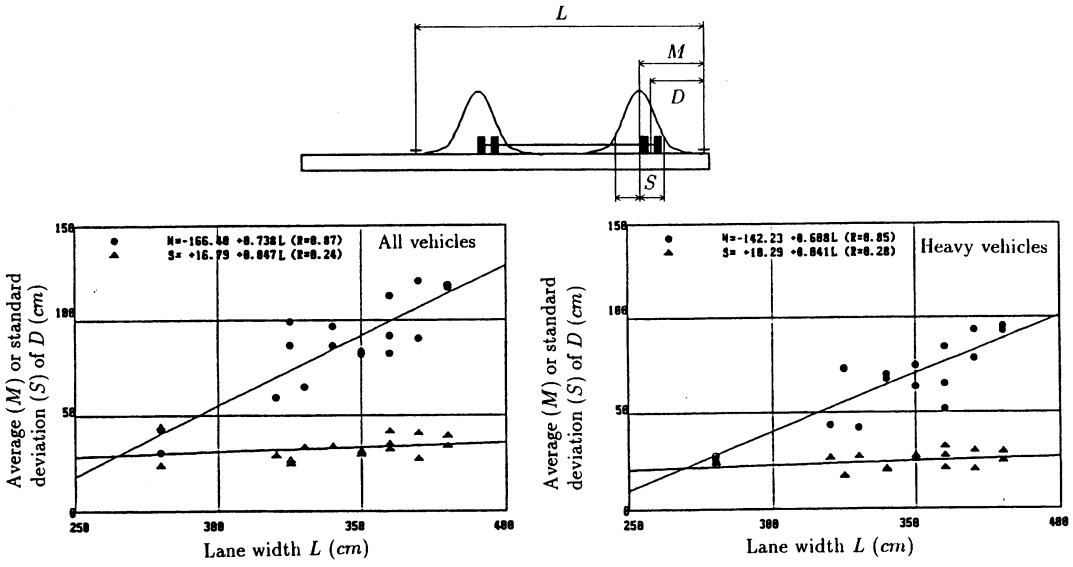


Figure 7: Parameters of lateral distribution of wheels and lane width

For all vehicles:

$$M = -166.40 + 0.738 \cdot L \quad (R = 0.87) \quad (1)$$
$$S = 16.79 + 0.047 \cdot L \quad (R = 0.24) \quad (2)$$

For heavy vehicles:

$$M = -142.23 + 0.608 \cdot L \quad (R = 0.85) \quad (3)$$
$$S = 10.29 + 0.041 \cdot L \quad (R = 0.28) \quad (4)$$

where
M : average of D as defined in Figure 7 (cm)
S : standard deviation of D (cm)
L : lane width (cm)
R : correlation coefficient

From these equations, it can be said that standard deviation of D has not correlation with lane width and is almost constant; $S \approx 30cm$ for all vehicles and $S \approx 23cm$ for heavy vehicles. By using these equations, the lateral distribution of wheels of heavy vehicles can be determined for any lane width if the distance between right and left wheels is assumed to be the average value of $1.9m$.

FEM ANALYSIS OF CONCRETE PAVEMENT

Outline of FEM analysis

In order to take into account of structural and wheel load conditions such as slab geometry, joint detail and lateral distribution of wheel loading, plate-FEM model is employed in this study. In the model, concrete pavement slabs are divided to rectangular plate elements and the mechanical effect of subbase is considered as the reaction force proportional to the deflection (Winkler foundation). Joints are modeled by joint elements based on the combined model proposed by the authors [4]. Based on FEM formulation, the stiffness equation for concrete pavement is given as follows:

$$\{f\} = [[K] + [J] + [H]] \cdot \{d\} \quad (5)$$

where
$\{f\}$: external force vector
$[K]$: stiffness matrix of concrete slab
$[J]$: stiffness matrix of joint
$[H]$: stiffness matrix of subbase
$\{d\}$: displacement vector

Wheel loads are assumed to be uniformly distributed over rectangular elements and incorporated into $\{f\}$. $[K]$ is a function of the slab geometry and the elastic properties of concrete. $[J]$ is based on the combined model which considers the effect of dowel bars and the aggregate interlock of joints. $[H]$ is a diagonal matrix and its components are a function of the subbase reaction modulus or K-value. Considering the boundary conditions and solving Eq.(5) for $\{d\}$, we can obtain stresses in concrete slab.

Table 1: Input data for influence line calculation

Slab width	$450cm, 375cm$
Slab thickness	$25cm$
Elastic modulus of concrete	$300,000kgf/cm^2$
Poisson ratio	0.2
K-value of subbase	$7.0kgf/cm^3$
Joint opening	$0.1cm$
Diameter of dowel bar	$2.5cm$
Length of dowel bar	$70cm$
Spacing of dowel bars	$40cm$
Wheel load	$8000kgf$
Contact area of wheel load	$30 \times 30cm$

Note: $1kgf/cm^2 = 0.098MPa, 1kgf/cm^3 = 9.8MPa/m$

Influence line of flexural stress

Since concrete slab is divided by transverse and longitudinal joints, stress condition in concrete slab depends on slab geometry and lateral distribution of wheel loading. Wheel loading on a transverse joint cause flexural stress at the transverse edge. When the slab width is small and wheel loading is near the longitudinal joint edge, flexural stress occurs at the longitudinal edge. These stresses accumulate fatigue and finally cause cracks of the concrete slab. Accordingly, the phenomena of cracking strongly depends on lateral distribution of wheel loading and geometry of the concrete slab.

In order to take into account of the lateral distribution of wheel loading in fatigue analysis , influence line of flexural stress of the concrete slab should be made. Figure 8 shows influence lines calculated by plate-FEM model using data as shown in Table 1. In Figure 8, the ordinate is flexural stress of concrete slab and the abscissa is the distance from the slab edge. The upper figures show influence lines of longitudinal flexural stresses along the transverse line at the midpoint between transversal joints. These influence lines can be used to estimate fatigue damage relating to transverse cracking. The lower figures show those of transverse flexural stresses along the transverse joint edge. They can be used to estimate longitudinal cracking starting from the transverse joint edge.

From the figures, it can be seen that the maximum longitudinal flexural stress is larger at the edge than at the interior, whereas transverse flexural stress is larger at the inner part than near the corner. This means that transverse fatigue cracks would occur if many heavy wheels pass near the longitudinal joint edge, whereas, if these wheels pass at the inner part of the lane, longitudinal fatigue cracks would occur

The maximum transverse flexural stress is larger in the case of 4.5m width slab than that of 3.75m, and the maximum longitudinal stress is almost the same in both slab widths. That is, slab width is effective to the transverse flexural stress. Since the occurrence of transverse and longitudinal cracks depends on the slab width, fatigue analysis should be conducted for both cases.

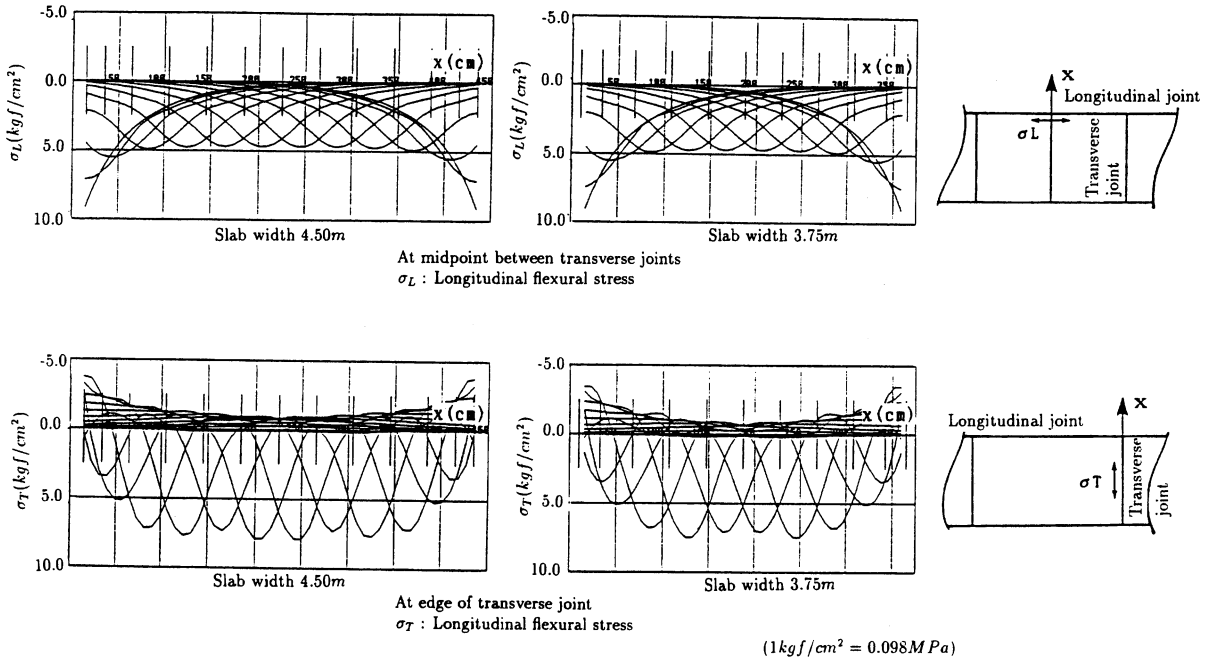


Figure 8: Influence lines of flexural stress

FATIGUE ANALYSIS

Fatigue damage

In the fatigue analysis of concrete pavement, combined stress of wheel load stress and thermal stress should be obtained and, then, the fatigue damage of concrete slab is estimated based on Miner's law. In this study, the fatigue damage is defined as follows:

$$F_d = \sum_i \frac{n_i(\sigma_i)}{N_i(s_i)} \tag{6}$$

where

F_d : fatigue damage
$n_i(\sigma_i)$: frequency of combined stress $\sigma_i = \sigma_p + \sigma_t$
σ_p : wheel load stress
σ_t : thermal stress
$N_i(s_i)$: stress repetition to failure at stress level $s_i = \sigma_i/\sigma_a$
σ_a : flexural strength of concrete

$N_i(s_i)$ represents the fatigue characteristics of concrete. Many studies have provided various equations which relate $N_i(s_i)$ to stress level s_i, however, in this study, the following equation is employed:

$$s = 1.082 - 0.0541 \cdot \log N \tag{7}$$

where

s : stress level
N : stress repetition to failure

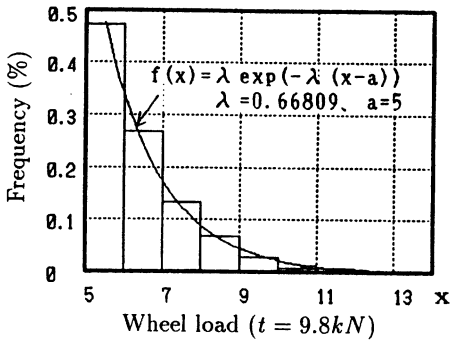


Figure 9: Distribution of wheel loads

Eq. (7) was derived at the probability of failure of 50 % based on the experimental result by Koyanagawa et al [5].

Wheel load stress

Histogram of wheel load stress can be obtained by means of the influence line of stress, the lateral distribution of wheels and the wheel load distribution. As discussed in the previous section, the lateral distribution of wheels can be determined, if the lane width is given. The distribution of wheel loads larger than 5t is modeled as a shift-exponential equation as shown in Figure 9. Parameters λ and a were derived from the data by Public Works Research Institute, Ministry of Construction [6].

Thermal stress

Thermal stress considered in this study is defined warping stress due to temperature gradient through concrete slab depth. The temperature gradient causes a convex or a converse curl of the slab. Since the weight of the slab restrains the deformation, the flexural stresses occur in the slab. The thermal stresses can be calculated by the following equation derived by Iwama based on the experiments [7]:

$$\sigma_t = 0.35 \cdot C_w \cdot \alpha \cdot E \cdot \theta' \tag{8}$$

where

σ_t : thermal stress
C_w : restraining coefficient of concrete slab
α : thermal expansion coefficient of concrete
E : modulus of elasticity of concrete
θ' : temperature gradient in concrete slab

Value of C_w is a function of slab length or joint spacing. Frequency of thermal stress, σ_t, is correspond to the frequency of θ', which is determined according to whether the difference of daily temperature is more than 14 $°C$ or not. The detailed calculation procedure of the frequency of σ_t is presented in the reference [1].

Procedure

Fatigue analysis is conducted as follows:

1. Input following data:
   (a) service years
   (b) lane width
   (c) volume of heavy vehicles (vehicles/day/lane)
   (d) distribution of wheel load as shown in Figure 9
   (e) geometry of concrete slab
   (f) elastic properties of concrete, E
   (g) flexural strength of concrete, σ_a
   (h) thermal coefficient of concrete, α
   (i) fatigue curve as presented in Eq. (7)
   (j) K-value
   (k) joint type. If dowel is used, its diameter, length and spacing are required.
   (l) temperature conditions or frequency data of temperature gradient in concrete slab in a year
2. Estimate a total number of wheels of heavy vehicles for service years, N_{all}.
3. Calculate frequency of σ_p, f_p, using influence line of stress, lateral distribution of wheels which can be determined from the lane width and distribution of wheel load.
4. Calculate frequency of σ_t, f_t, according to the procedure as presented in the previous section.

Table 2: Input data for Kaga pavement

Slab width	$450cm$
Slab thickness	$23cm$
Flexural strength of concrete	$45kgf/cm^2$
Elastic modulus of concrete	$300,000kgf/cm^2$
Poisson ratio	0.2
K-value of subbase	$7.0kgf/cm^3$
Joint opening	$0.1cm$
Diameter of dowel bar	$2.5cm$
Length of dowel bar	$70cm$
Spacing of dowel bars	$40cm$
Service years	25 years
Lane width	$350cm$
Volume of heavy vehicles	2,200 vehicles/day/lane
Spacing of transverse joints	$6m$
Thermal expansion coefficient of concrete	$10 \times 10^{-6}/°C$
Temperature condition	Difference of daily temp. $< 14°C$

Note: $1kgf/cm^2 = 0.098MPa, 1kgf/cm^3 = 9.8MPa/m$

5. Calculate frequency of $\sigma_i = \sigma_p + \sigma_t$, f_i as follows:

$$f_i = f_p \cdot f_t \tag{9}$$

6. Estimate increment of fatigue damage at stress level $s_i = \sigma_i/\sigma_a$ as follows:

$$\begin{aligned} \delta F_d &= \frac{\delta n_i(\sigma_i)}{N_i} \\ &= \frac{N_{all} \cdot f_i}{N_i} \end{aligned} \tag{10}$$

where N_i can be calculate for stress level s_i by Eq. (7).

7. Repeat from 1 to 6 for all stress level and estimate total fatigue damage according to Eq. (6)

CASE STUDIES

Relationship between fatigue damage and cracking

Concrete pavement of National Highway Route 8, Kaga Ishikawa, was constructed 25 years ago. A lot of longitudinal cracks have been observed in this pavement. Fatigue analysis was conducted to study the relationship between fatigue damage and cracking of the pavement. Table 2 shows the input data for this analysis based on the design detail of this pavement.

Figure 10 shows the relationship between frequency of stress level, lateral distribution of wheels of heavy vehicles and fatigue damage along transverse joint. In this case, center line coincides with the longitudinal joint as in the general

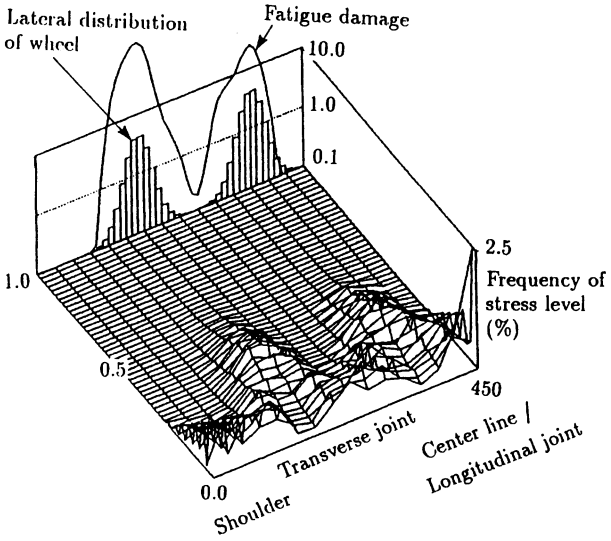


Figure 10: Result of the fatigue analysis

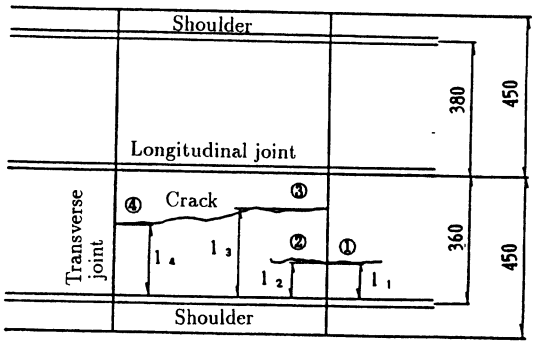


Figure 11: Condition survey of cracking

way. The axis of ordinate of fatigue damage is shown by logarithmic scale. Along the wheel paths of heavy vehicles, two peaks of frequency of stress level can be seen in this three dimensional graph. The phenomenon strongly contributes to the accumulation of fatigue damage.

Actually, this pavement has a lot of longitudinal cracks. In order to find the relation between cracking and fatigue damage, visual condition survey was conducted. In the survey, positions of longitudinal cracks at the transverse joints were measured as shown in Figure 11, and obtained frequency of longitudinal cracks.

Figure 12 shows the histogram of longitudinal cracks and the fatigue damage calculated above. It can be seen that the fatigue damage calculated well corresponds to the frequency of cracks. This means that fatigue damage can be used as an indicator of the occurrence of crack. However, it should be noted that the structural condition of the pavement is changed because of the cracking. Therefore, the fatigue analysis should be conducted based on the "post-cracking" condition. Accordingly, further study should be required about quantitative relationship between the fatigue damage and the possibility of cracking.

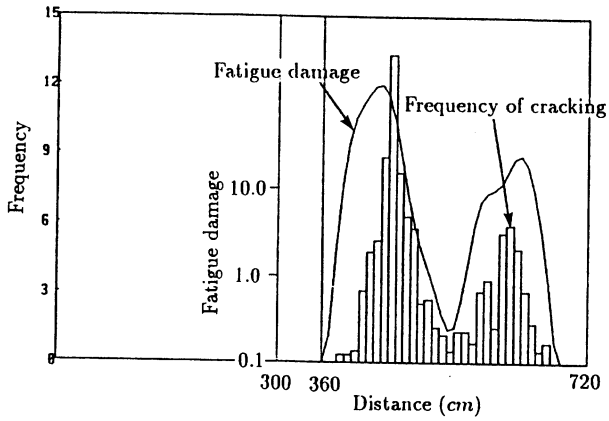


Figure 12: Frequency of longitudinal cracks

The effect of slab geometry on cracking

In order to study the effect of slab geometry, that is, lateral distribution of wheels on fatigue damage of concrete pavement, fatigue analysis was conducted by varying lane widths shown in Table 3.

Calculations were conducted at the midpoint between the transverse joints for transverse cracking and at the transverse joint edge for longitudinal cracking.

Figure 13 gives some examples of the results. The figure shows the relationships between frequency of stress level, lateral distribution of wheels, and fatigue damage. Figures in the upper part are the results for the transverse crack at midpoint between the transverse joints and figures in the lower part are for the longitudinal crack at the transverse joint edge. Fatigue damage for the transverse crack exceeds 1.0 at the longitudinal joint edge, in the case of the slab width being small ($3.75m$). On the other hand, in the case of the slab width being large ($4.5m$), fatigue damage for the longitudinal crack exceeds 1.0 in the wheel paths.

Figure 14 shows the relationship between fatigue damage and slab width as a parameter of lane width. From this figure, it can be said that, when the slab width and lane are small, fatigue damage for the possibility of transverse cracking at the midpoint between the transverse joints is greater than that for the possibility of the longitudinal cracking at the transverse joint edge. On the contrary, when the slab width is large, the tendency becomes reverse. This tendency corresponds to the results of the investigation previously conducted in Japan [8]. This paper reports that longitudinal cracks have been more frequently observed in concrete pavements with wider slabs. At the midpoint between transverse joints, the effect of lateral distribution of wheels, which is related with lane width, on the fatigue damage is significant

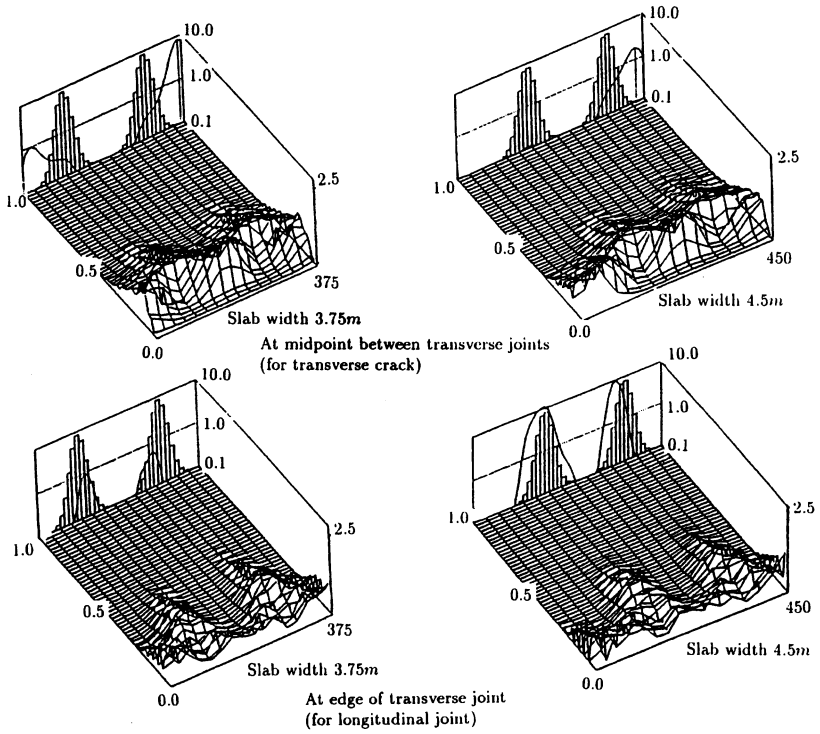


Figure 13: Effect of slab width (lane width: 3.5 m)

Table 3: Input data for the effect of slab width

Slab width	$375cm, 400cm, 450cm$
Slab thickness	$25cm$
Flexural strength of concrete	$45kgf/cm^2$
Elastic modulus of concrete	$300,000kgf/cm^2$
Poisson ratio	0.2
K-value of subbase	$7.0kgf/cm^3$
Joint opening	$0.1cm$
Diameter of dowel bar	$2.5cm$
Length of dowel bar	$70cm$
Spacing of dowel bar	$40cm$
Service years	25 years
Lane width	$325cm, 350cm$
Volume of heavy vehicles	2,200 vehicles/day/lane
Spacing of transverse joints	$6m$
Thermal expansion coefficient of concrete	$10 \times 10^{-6}/°C$
Temperature condition	Difference of daily temp. $< 14°C$

Note: $1kgf/cm^2 = 0.098MPa, 1kgf/cm^3 = 9.8MPa/m$

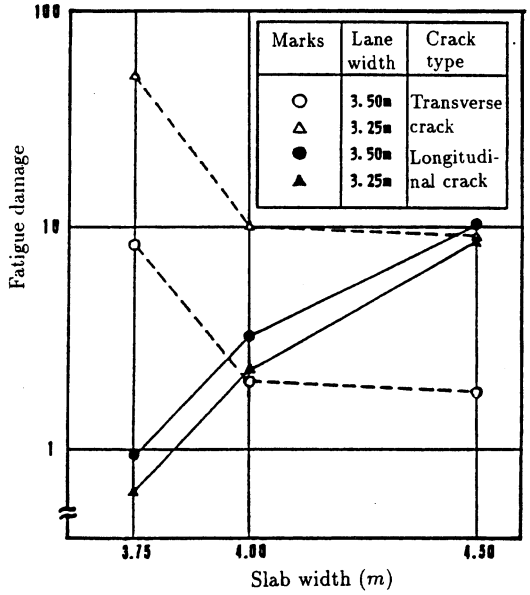


Figure 14: Effects of widths of slab and lane

for the transverse cracks. This is because the frequency of the wheels passing near the longitudinal joint edge increases as slab width or lane decrease. Furthermore, longitudinal flexural stress due to wheel loading is much larger at the longitudinal joint edge. On the other hand, fatigue damage at the transverse joint edge for longitudinal crack is not so affected by lateral distribution of wheels. This is because the standard deviation or the degree of the concentration of wheels is not affected by lane width.

CONCLUSIONS

It is generally accepted that the lateral distribution of wheels, particularly, of heavy vehicles, significantly affects on the cracking of concrete pavements. In order to measure the distribution of wheel passing without disturbing traffic flow, a portable measuring system named TLAMS was developed.

Lateral distribution of wheels was modeled based on the measuring results by TLAMS. Normal distribution is applied to this model. It was shown that the parameters of the function are linearly related to lane width.

Fatigue analysis was conducted to study the effects of lateral distribution of wheels on fatigue cracking. In the fatigue analysis, influence lines of flexural stress were obtained by plate-FEM analysis and fatigue damage was calculated based on Miner's law.

From the fatigue analysis of Kaga Ishikawa concrete pavement, good correspondence between the fatigue damage calculated and the fatigue cracking observed was shown. Numerical calculations were conducted on various types of concrete pavements and the effects of lateral distribution of wheels were also investigated. The results of the calculations showed that transverse crack would occur at the midpoint between transverse joints in the case of narrow slab, whereas longitudinal crack would occur at the transverse joint edge in the case of wider slab. These results correspond well to the investigation previously conducted in Japan.

References

[1] Manual of Cement Concrete Pavement, Japan Road Association, 1984.

[2] Thickness Design for Concrete Highway and Street Pavements, Portland Cement Association, 1984.

[3] Kajikawa, Y., Nishizawa, T. and Sugimoto M., Development of Portable Traffic Flow Measuring System, Proceeding of JSCE, No. 391/VI-8, pp. 107–114, 1988. (in Japanese)

[4] Nishizawa, T., Fukuda, T., and Matsuno, S., A Refined Model for Doweled Joints of Concrete Pavements Using FEM Analysis, Proceedings of Fourth International Conference on Concrete Pavement Design and Rehabilitation. pp. 100-110, 1989,

[5] Koyanagawa, M., Kokufu, K. and Fukuda, T., A Basic Study on the Flexural Fatigue of Concrete Pavement Slab, Proceeding of JSCE, No. 372/V-5, pp. 131–137, 1986. (in Japanese)

[6] Iijima, N. and Imai, H., Results of Condition Survey of Heavy Vehicle Loads and Its Application to Pavement Design, Technical Note of Civil Engineering, Vol. 24-2, 1982. (in Japanese)

[7] Iwama, S., Experimental Studies on the Structural Design of Concrete Pavement, Report of Public Works Research Institute, Ministry of Construction, Vol. 117, 1964. (in Japanese)

[8] Fukuda, T., Koyanagawa, M. and Murai S., Condition Survey of Concrete Pavements and Its Evaluation, Proceedings of Third International Conference on Concrete Pavement Design and Rehabilitation, pp. 519–523, 1985.